


Article

# Validating Sea-Level Altimetry Data against Tide Gauge for Coastal Risk Analysis in Mozambique

Fialho Paloge Juma Nehama <sup>1,\*</sup> , Zeinul Dufa Hassane Veriua <sup>1</sup>, Clousa Maueua <sup>2</sup>, Angela Hibbert <sup>3</sup> , Francisco Calafat <sup>3</sup>  and Peter David Cotton <sup>4</sup>

<sup>1</sup> Escola Superior de Ciências Marinhas e Costeiras, UEM, Quelimane P.O. Box 128, Mozambique

<sup>2</sup> Instituto Nacional de Hidrografia e Navegação, Maputo P.O. Box 2089, Mozambique

<sup>3</sup> National Oceanography Center, Joseph Proudman Building, 6 Brownlow Street, Liverpool L3 5DA, UK

<sup>4</sup> Satellite Oceanographic Consultants Ltd., 49 Seal Road, Stockport SK7 2JS, UK

\* Correspondence: fialho.nehama@uem.ac.mz

**Abstract:** Satellite altimetry data provide a solution to the lack of in situ tide gauge data, which are essential for comprehending various marine processes worldwide. In the present study, we seek to validate ALES-retrieved sea-level data against tide gauge observations from four ground stations on the coast of Mozambique. The approach consisted of extracting data from selected tracks of the Jason-1, Jason-2 and Jason-3 missions, and processing it to (i) remove outliers, (ii) collocate alongside tide gauge data, (iii) remove the tidal component and detrend, and (iv) perform a set of statistical analyses. Good agreement was found between the altimetry and tide gauge data in three of the four stations (Maputo,  $r = 0.59$ ; Inhambane,  $r = 0.87$ ; and Pemba,  $r = 0.75$ ), with the exception of Beira. The annual and semi-annual cycles in the two datasets revealed that the altimetry signal is smaller in amplitude and ahead (with a few exceptions) of tide gauge by a varying number of days in each location. Both the annual and semi-annual cycles are far more comparable in Pemba, where the amplitude in particular has the same order of magnitude, followed by the Maputo station. The study concluded that the selected altimetry data for Pemba and Maputo stations are valid and can be used for coastal risk analysis and other applications. No altimetry data could be validated for Inhambane and Beira stations due to lack of consistent and sufficiently long tide gauge records. This difficulty urges the need for improved maintenance practices of ground stations located near human settlements that rely on sound information of the sea level and its variability to protect lives, infrastructure and livelihoods.

**Keywords:** sea level; coastal risk; satellite altimetry; algorithm; ALES re-tracker



**Citation:** Nehama, F.P.J.; Veriua, Z.D.H.; Hibbert, A.; Maueua, C.; Calafat, F.; Cotton, P.D. Validating Sea-Level Altimetry Data against Tide Gauge for Coastal Risk Analysis in Mozambique. *J. Mar. Sci. Eng.* **2022**, *10*, 1597. <https://doi.org/10.3390/jmse10111597>

Academic Editor: Wei-Bo Chen

Received: 8 September 2022

Accepted: 1 October 2022

Published: 29 October 2022

**Publisher's Note:** MDPI stays neutral with regard to jurisdictional claims in published maps and institutional affiliations.



**Copyright:** © 2022 by the authors. Licensee MDPI, Basel, Switzerland. This article is an open access article distributed under the terms and conditions of the Creative Commons Attribution (CC BY) license (<https://creativecommons.org/licenses/by/4.0/>).

## 1. Introduction

Sea-level rise poses a threat to many coastal communities around the globe. It is expected that a rise of 90 cm during the current century will endanger at least 100 million people, cities, ports and wetlands located in low-lying coastal regions by means of increased coastal inundation, erosion and salt intrusion [1,2]. Until recently, precise estimates of sea level fluctuations were not readily available in most coastal sites where risks need to be monitored, partly due to problems associated with the use of tide gauges. According to [3,4], these problems include the poor geographic distribution of tide gauges with a long period of observations, the discontinuity in time series of available data, since they come from different equipment over time, and the contaminations that arise from the fact that tide gauge measures sea level in relation to the structure in which it is installed; that is, observations contains signals from crustal movements or local structural changes that are otherwise assumed to be variations in absolute sea level. With the advent of satellite altimetry in the early 1990s, changes in absolute sea level can be estimated worldwide with unprecedented accuracy, thanks to the satellite's frequent sampling capability and

global coverage. Additionally, over the last two decades, satellite altimetry has been effectively used to monitor a number of coastal hazards, including coastal flooding, erosion, coastline movement, maritime security, marine pollution, water quality, marine ecology shifts, several marine biophysical features and atmospheric and oceanic drivers of change. See [5] for a concise review of satellite remote sensing of marine coastal hazards.

On the other hand, coastal altimetry evolved considerably over the years to overcome issues often associated with the precise estimation of geophysical parameters along the land–sea interface. A detailed review of the major technical improvements made so far is presented in [6], and it includes the coastal-specific data editing approaches, the revised algorithms for key corrections to the basic retrieved data, and the use of new schemes for radar echo analysis, also known as re-tracking. The latter is a process that consists of fitting a model to the real signal received by a satellite, also called a waveform. Known re-tracking algorithms include (i) those that use the shape of waveform and some functional form to perform the fitting and the subsequent waveform classification, (ii) those that employ an empirical model of the waveform, (iii) those that process a stack of successive waveforms in order to remove spurious echoes, and finally (iv) those that perform the fitting of a small portion of the waveform (sub-waveform) containing the leading edge, but ignore the trailing edge [6,7]. The Adaptive Leading-Edge Sub-waveform (ALES) re-tracker, first presented in [7], is one such algorithm, in which selected parts of the returned echo are modeled with the “open ocean” Brown functional form. The result is the retrieval of more coastal waveforms compared to the classic processing, without compromising the accuracy of the standard processing for open ocean and coastal regions. The standard processing would often fail in coastal areas due to land contamination, as measured by the radar altimeter microwave radiometers, and the consequent signal degradation of the wet tropospheric correction, determined by measurements and errors in global tide models.

Coastal areas worldwide represent huge social, biological, and economical value, as they are home for a vast majority of the population in coastal states. They also aggregate the most productive ecosystems, which are often composed of a combination of marine and terrestrial fauna and flora, and provide services of elevated social and economic importance. The coast of Mozambique is the country’s most valuable natural resource and comprises a variety of habitats, including the coral reefs, swamps, and sandy beaches and coastal dunes that provide goods and services for nearly 60% of the country’s population, inhabiting the coastal zones. Resources and natural capital along the Mozambican coast are highly vulnerable to the consequences of climate variability and change, mostly due to the combination of the inherent dynamic nature of coastlines and exposure to marine hazards, inefficient land usage, strain on natural resources, tropical cyclones, and sea-level rise [1,8–10]. Being able to protect coastal communities and safeguard economic activities relies on availability and access to regional information on coastal risk factors such as wave and wind extremes, surface currents, and sea level. In particular, changes in sea level are primarily estimated from high-frequency tide gauge (TG) records, and Mozambique has a network of stations consisting of thirteen coastal stations, four of which (Maputo, Inhambane, Nacala and Pemba) provide quality controlled data and were operational for a considerable amount of time following their installation [11]. The tide observations in this network are subjected to the classical limitations [12], which are aggravated when monitoring sea level in the least developed countries with inadequate capabilities for maintaining TG networks (including the supply of spare parts, and prompted data delivery).

Using TG data in combination with satellite altimetry data to overcome the associated sampling and processing issues [5] requires validation of the algorithms. This is accomplished by comparing two different amounts comprising different signals of sea level with inevitable space and time separation between them. The spatial separation arises from the fact that consecutive satellite ground tracks are  $\sim 20$  km apart and are not coincident with TG locations in the coast. This issue is far more concerning than the time separation, which arises from the fact that satellites revisit a location every 9.915642 days at best, while TG

measures at higher frequency (usually every hour), and therefore the timestamp will most likely be different in each of these observations.

In this study, we seek to compare altimetry data processed with the ALES re-tracker against TG records from four ground stations located along the coast of Mozambique, as a step towards monitoring sea-level changes, coastal risk analysis and prediction, and using altimetry data for other coastal applications. The distance from altimeter to the sea surface, also termed the altimeter range, estimated using ALES has been previously validated by means of comparison with TG records in different regions of the world [13,14]; here, the validation is extended to the coastal waters in the western margin of the Mozambique Channel. Our goal was to evaluate the quality of altimeter-based sea surface height anomalies (SSHA).

## 2. Materials and Methods

### 2.1. Study Area

Mozambique Channel (Figure 1) lies between the African continent and its largest island, Madagascar, in the western Indian Ocean, a region of intense dynamical exchange of oceanic water masses originated in the Atlantic, Antarctic, and Indian oceans. The oceanic circulation within the channel is dominated by a number of large (>300 km wide) and highly variable anticyclonic eddies propagating poleward. Under the south-going surface current, the trajectory of water masses flowing north follows the seabed topography, characterized by oceanic ridges and plateaus. The wind regime is seasonal and strongly influenced by the movement of the Inter-Tropical Convergence Zone [10], and the channel is known to host almost two tropical storms or cyclones per year, regardless of whether these were originated elsewhere and traveled into the channel, or whether they formed within the channel [15]. Tropical cyclogenesis conditions have been observed in the Mozambique Channel [13,15], which include high SSTs (29.6 °C on average), a southerly wind shear with height, and below-normal geopotential height anomalies at 500 hPa. However, there are more tropical storms or cyclones that enter the channel than those originated there, and about half of the latter make landfall at either the African mainland or Madagascar. The maximum sustained winds during the passage of a tropical storm or cyclone is associated with a minimum sea-level pressure, and when combined, the two induce disturbances of the sea surface height, often called a storm surge [16], which is also present in the signal retrieved by altimetry.

The amplitude of the semi-diurnal astronomical tides increases gradually from each end towards the central part of the channel [17]. These characteristics drive a complex system of coastal currents [18], local upwelling [19,20], lee eddies [21] and internal tides [22].

Four study areas (shown in Figure 1) in the western margin of the Mozambique Channel were selected to validate the altimetry data from ten tracks of the Jason series of satellites that were made available. Maputo, which lies landward in the Delagoa Bight, is a small, shallow and rectangular bay with maximum depth, width and length of 15 m, 15 km and 96 km, respectively. The tidal amplitude is amplified from 2 m at the entrance to 3.5 m at the inner boundary [23–25]. The TG in Maputo is located inside a large bight, at the northern margin of Espirito Santo estuary. The closest satellite track is the #70, which reaches the land at some distance away from the TG station, such that the satellite measurements of sea level might not precisely represent conditions inside the Maputo Bay. Track #5 is located mostly on the coast, with some stretch crossing diagonally the Maputo Bay.

Inhambane Bay is a bifurcated two-channel bar-built estuary with an along-coast channel of 30 km and a secondary channel of 12 km [26]. The Inhambane TG station is nearly at the center of a satellite track grid, resulting in large distances between TG and satellite measurements. In addition, validation at this station is hampered by the short time series of data available from the tide gauge (about 300 days in 2011).

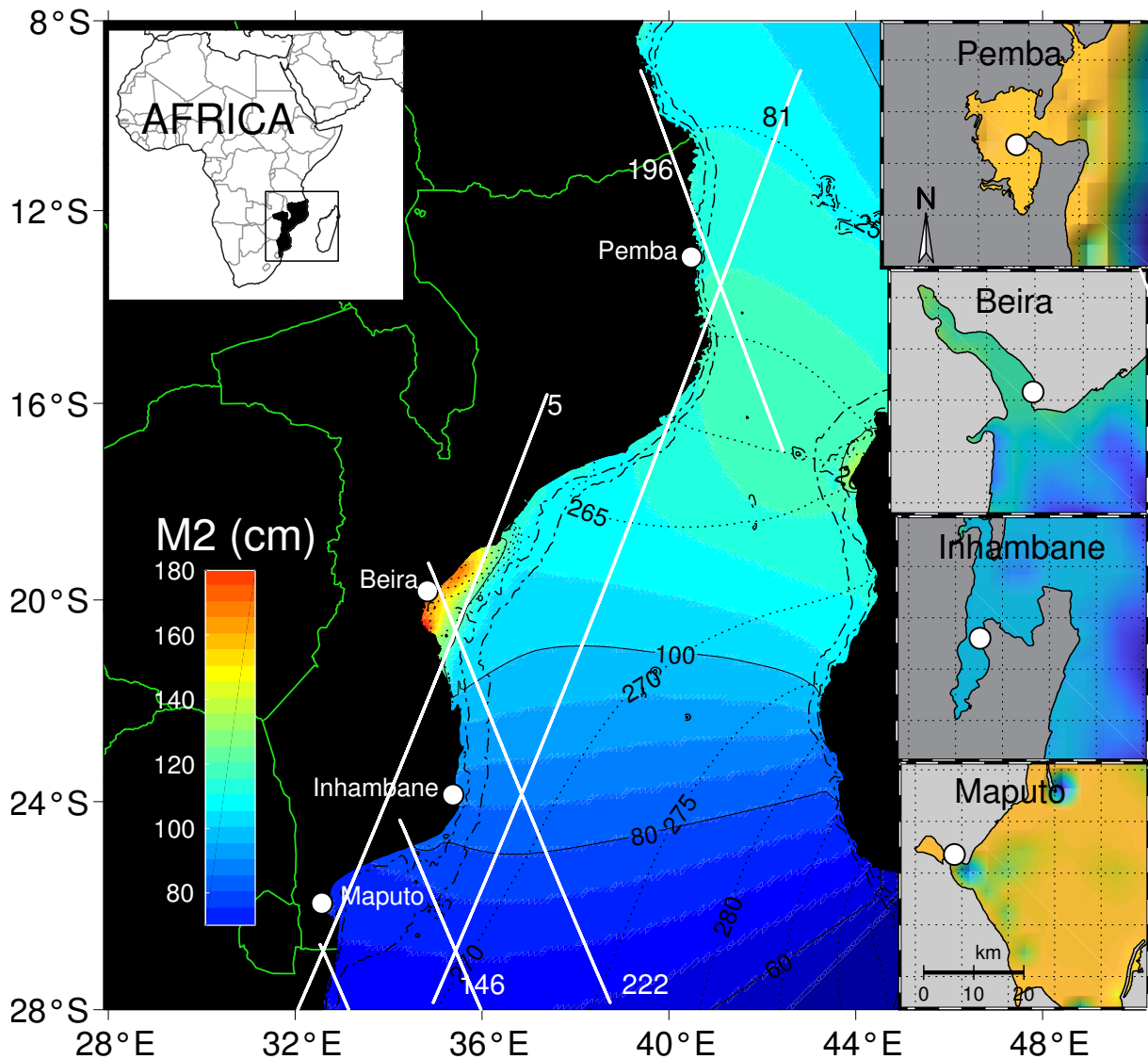


**Figure 1.** Map showing the study area, and the location of TG (white dots) and its nearest satellites tracks (white lines). The map also shows the distribution of  $M_2$  tidal amplitude (colors) and phase in degrees (dotted contours) in the Mozambique Channel, based on data from the Oregon global model v7. Bathymetry contours of 100 m and 1000 m are also plotted to indicate the position of the shelf edge. Colors in the inset maps illustrate bathymetric changes.

The Beira estuary is a shallow body of water, with a maximum depth of 10 m. The geomorphological conditions are associated with the active abrasion and sedimentation of coastal and fluvial–marine environments, with emphasis on flooded areas or those under seasonal tidal dominance [27]. The TG station is located in harbor zone, and the satellite track 222 crosses the land very close to the TG station.

Pemba harbor is located in a semi-enclosed basin in northern Mozambique. There are claims that it is the world’s third deepest bay and Africa’s deepest. According to [28], the tide propagation along the coast has a phase lag of about 30 min, reaching Pemba TG station first and then Quelimane, Maputo and Beira. In Pemba, tracks 81 and 196 are located near the tide gauge, and the data for both passes give correlations greater than 70%. Another advantage apart from the long record in Pemba is the coastal geometry that encompasses a coastline oriented directly to the North, and there are no embayments with considerable dimensions or shoaling environments. Under such conditions, the offshore sea-level signal is likely to be well linked to the coastal sea level.



### 2.2. Datasets

Radar altimetry data from three high-precision altimetry missions, Jason-1, Jason-2, and Jason-3, were used in this study. The Jason-1 mission (Dec 2001 to Jul 2013) was launched by the National Aeronautics and Space Administration (NASA) and the Centre National d'Études Spatiales (CNES) to ensure continuity of oceanographic observations from the earlier Topex/Poseidon mission. The satellite carries the Poseidon-2 altimeter operating at Ku (13.575 GHz) and C (5.3 GHz) bands. The Jason-2 (Jun 2008 to Dec 2020) was launched as a cooperation involving CNES, NASA, the National Oceanic and Atmospheric Administration (NOAA), and EUMETSAT. Jason-2 carries the Poseidon 3, a two-frequency solid-state radar altimeter that accurately measures distance from the surface and also provides ionospheric corrections with about 2 cm precision. Jason-3 is the follow-on altimetry mission of Jason-2/OSTM (launched 17 January 2016) led by the operational agencies: NOAA, EUMETSAT, and CNES. All these Jason-series satellites are on a 10-day repeating orbit, flying at 1336 km above the Earth, covering all oceanic and continental surfaces located between 66° N and 66° S.

The ALES re-tracker was applied to the dataset from Jason series by the UK's National Oceanographic Center (NOC) to produce customized datasets for the Coastal Risk Information Service project (C-RISe; [www.c-rise.info](http://www.c-rise.info)), which comprises the along-track coastal geophysical data records (CGDR), subsampled at 20 Hz for a selected region of the western Indian Ocean. The C-RISe data are made of all standard Jason products covering the period from January 2002 to September 2016, in addition to sea surface height anomaly (SSHA) relative to DTU15 mean sea surface [29], and a range of supplementary parameters and relevant auxiliary geophysical corrections.

Tidal data used in this study as fiducial reference measurements were obtained from the Mozambican National Institute for Hydrography and Navigation (INAHINA; [www.inahina.gov.mz](http://www.inahina.gov.mz)) network of tide gauges. We used data from four tide gauge stations (Table 1) covering the northern, central and southern coast of Mozambique. The data are archived in two places: the University of Hawaii Sea level Center (UHSLC; <http://uhslc.soest.hawaii.edu>, (accessed on 15 April 2019)), and the Intergovernmental Oceanographic Commission Sea Level Station Monitoring Facility (IOC SLMF; [30]).

**Table 1.** Coordinates of the tide gauge stations. Column 4: time interval used for validation in Julian day/year format. Column 5: satellite tracks that lie within 300 km from TG location.

TG Station	Latitude (°)	Longitude (°)	Validation Period	Satellite Tracks	Datum	Source
Maputo	−25.97	32.57	1/2002–366/2004	570,146	2.17	IOC SLMF
Inhambane	−23.87	35.38	66/2011–365/2011	5,146,222	5.31	UHSLC
Beira	−19.82	34.83	50/2002–365/2003	5222	3.57	IOC SLMF
Pemba	−12.97	40.48	109/2007–179/2013	81,196	2.32	UHSLC

Data from the UHSLC comprised total water levels and non-tidal residuals filtered to hourly intervals, and they were supplied in a quality-controlled format referenced to Chart Datum. The high-frequency data from IOC SLMF are available for sampling intervals of 1–3 min, and are similarly referenced to Chart Datum. Generally, each data point is an average of multiple samples collected during the sampling interval. These data were subsampled to hourly intervals, quality controlled and tidally analyzed using the NOC's Tide Analysis Software Kit (TASK).

### 2.3. Methods

This study aims to validate ALES retracked sea-level data for application in coastal risk monitoring in coastal zones of Mozambique, and to determine SSHA trends and statistics in four selected stations. A full description of the ALES coastal processor is given in [7]. The mere concept of data validation has been a topic of debate amongst researchers of various fields of knowledge. Taking into consideration the linguistic complexity and

immense possibilities of its meaning when using the term validation, for the purpose of this paper, we define data validation as the process of determining that a dataset possesses a satisfactory level of accuracy that is appropriate for its intended use [12]. The level of accuracy is chosen to be 60% for a domain of applicability that encompasses the data-poor coastal regions of Mozambique and the risk factors associated with sea level, while the intended use is the study of past and future hazardous events. The emphasis is on the qualitative validation of altimetry data, determined based upon the agreement of ALES outputs data and TG data.

In this study, we applied the validation procedures presented in [12] as a form of assessing the validity of altimetry data in the region of interest, using the following metrics: coefficient of variance (CV), bias, Pearson's correlation coefficient (R), root mean square difference (RMSD), and mean absolute error (MAE). The match-up validation protocol uses three steps, described as follows.

The first step consists of subsampling the TG data into hourly intervals, and tidally analyzing the time series using the TASK software, thereby removing the outliers. Given that the UHSLC data are a product of filtering and the IOC SLMF data were derived via subsampling, theoretically, the two are not directly comparable. The subsampled data are likely to give more realistic tidal amplitudes, whilst the filtered data should exhibit less noise. In practice, testing has shown that the TASK outputs vary little depending upon the sampling rate used. The in situ SSHA is defined as:

$$SSHA_{in\ situ} = h(t) - \overline{h(t)} \quad (1)$$

where  $h(t)$  is the instantaneous stage value in the gauge record at time  $t$  with the tides removed, and the overbar denotes ensemble average.

The second step is to extract SSHA from the standard C-RISe CGDR, which is an altimetry product that already includes all of the corrections indicated in Equation (1), with the exception of dynamic atmospheric correction (DAC), since tide gauge records are also affected by these atmospheric fluctuations. The altimetric SSHA is defined as [31–34]:

$$SSHA_{alt} = H - [R + \sum \Delta R_{Env} + (\Delta R_{Solid} + \Delta R_{Ocean} + \Delta R_{Atm})] - MSS \quad (2)$$

where  $H$  is the orbit altitude measured in reference to an ellipsoid,  $R$  is the altimeter range and  $MSS$  is the mean sea surface. The altimeter range represents the nadir distance taken from the center of mass of the satellite to the sea surface after considering instrument corrections, and a set of environmental ( $\sum \Delta R_{Env}$ ) and geophysical corrections. The latter accounts for vertical motions due to solid earth tide ( $\Delta R_{Solid}$ ), oceanic tides ( $\Delta R_{Ocean}$ ) estimated from the FES2014 Ocean Tide model and DAC ( $\Delta R_{Atm}$ ). The dynamic atmospheric correction is a model of the sea surface response to preceding time series of pressure and wind, and is estimated from a meteorological model [35]. It consists of both a simple "static" response to the atmospheric pressure at that time (also known as "inverse barometer correction"), and the high-frequency "dynamic" response to the history of changes in atmospheric pressure and winds.

The quality of a comparison can be affected by the amount and type of outliers. So, in order to avoid misleading results, outliers in altimetry SSHA were detected and excluded, by imposing that the excursion from the median SSHA should not surpass 2 m or the triple of standard deviation [33,34]. A filter was then applied to the altimetry SSHA by taking the median value of data points located within a certain radius from TG locations. The radius distance was chosen iteratively using 2.5 km increments in order to minimize the root mean square difference between altimetry and TG records. In agreement with [7,34], using the median value is a more robust approach in the presence of outliers than using the mean value. All data that had time separation with TG surpassing two hours were excluded from computations, and a temporal interpolation in TG observations was performed to match the time in both datasets.

The third step is the selection of an altimetry dataset that best agrees with TG data, and subsequent analysis of both time series in order to retrieve useful oceanographic information. The performance of altimetry datasets varies with the satellite passes, and also with the points along each pass. The selection was based on commonly reported statistics that rely on mean squared errors, such as correlation coefficient and root mean square difference, and additional metrics that rely on simple deviation, such as bias and mean absolute error. RMSD is a good metric for agreement between datasets with Gaussian distribution when their sensitivity to outliers is to be tested; however it fails to capture the average error when the dataset contains outliers [36]. In addition to RMSD, we use the mean absolute error (MAE) to support the dataset selection, since it correctly presents the error magnitude and does not amplify outliers. The correlation coefficient has recognized merit in assessing the goodness of fit involving remotely sensed and in situ data; nevertheless, it can report good values in strongly biased and low-precision datasets, leading to misinterpretation of results. Here, precision is assessed through the coefficient of variance (CV), which was calculated as the ratio of standard deviation to the mean SSHA. CV does not require collocation of satellite and in situ data, and gives an estimate of the intra-pixel stability and temporal consistency of the dataset. Star plots were generated at each TG location to visually inspect and compare the performance of altimetry data for the ten tracks, and points along passes gave the five best correlations with TG data. To that end, the values of bias, CV, RMSD, MAE and R were normalized to their range, resulting in metrics scaled from zero to one. Lower values for most of these metrics (except for correlation coefficient) indicate a better performance of the dataset, and by reversing the axis orientation, these metrics were switched to “visually reporting good performance” further away from the center in a star plot. The mathematical formulations of the various metrics discussed above are given in [37].

As per the case study in [6], the sea-level variability was further analyzed in terms of monthly means, and the annual and semi-annual cycles estimated by fitting the following curve to the de-tided SSHA data:

$$\hat{y}_t = a + bt + c \cos\left(\frac{2\pi}{365.24}t\right) + d \sin\left(\frac{2\pi}{365.24}t\right) + e \cos\left(\frac{4\pi}{365.24}t\right) + f \sin\left(\frac{4\pi}{365.24}t\right) + \epsilon_t \quad (3)$$

where the coefficients  $a$  through  $f$  can be estimated in regression analysis. In this study, the Bayesian multiple regression with auto-correlated errors was employed, along with the Gibbs sampling. The annual and semi-annual amplitudes  $A$ , and phases  $\Phi$  are calculated from:

$$A_{annual} = \sqrt{c^2 + d^2}; \quad A_{semi-annual} = \sqrt{e^2 + f^2} \quad (4)$$

and

$$\Phi_{annual} = \tan^{-1}\left(\frac{d}{c}\right); \quad \Phi_{semi-annual} = \tan^{-1}\left(\frac{f}{e}\right) \quad (5)$$

While amplitudes and phases give the basic characteristics of the SSH variability in annual and semi-annual frequencies, additional and useful information is provided by coefficients  $a$ ,  $b$  and  $\epsilon$ , representing bias, linear trend and error term, respectively. Depending on the time period under analysis, the trend can either give information on yearly variability if a shorter time-series is considered, or it can give an estimate of the sea-level change associated with climatic changes if a much longer time-series is used instead.

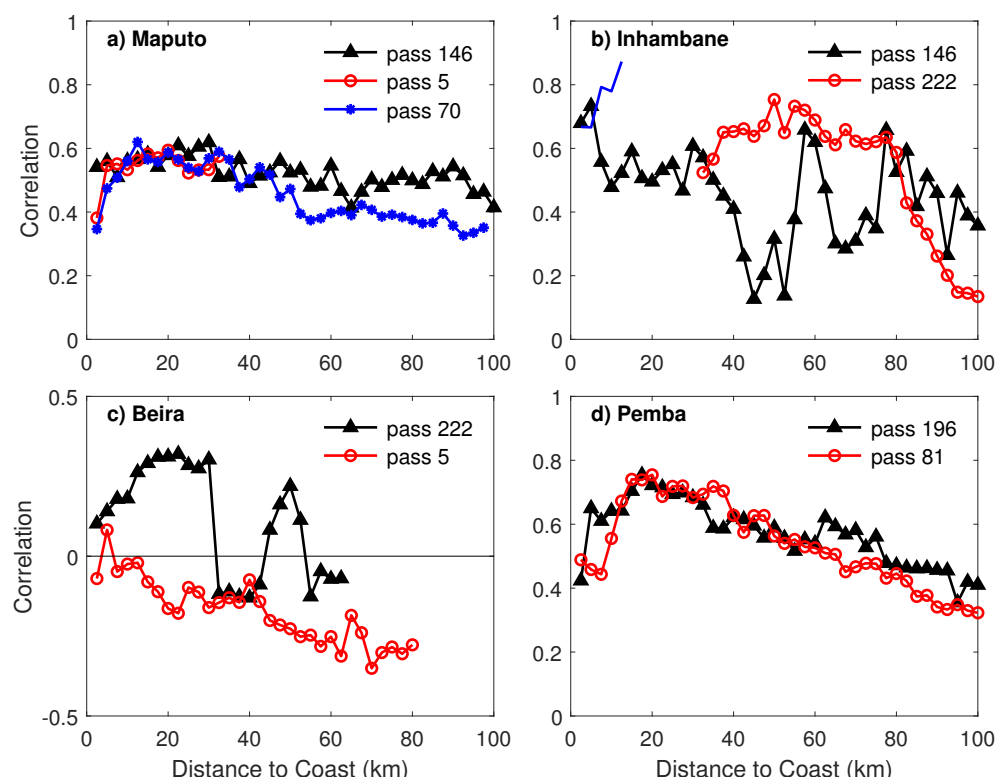
### 3. Results

#### 3.1. Selection of Satellite Tracks

Comparisons between satellite-derived data with tide gauge SSHA were performed at the four locations listed in Table 1. These stations were chosen because tidal records are the longest available in the country, and the data are acquired and maintained through a carefully controlled system, unlike the remaining tidal stations. For consistency with spacing of the Jason-series satellite ground tracks, only the altimetry passes located within

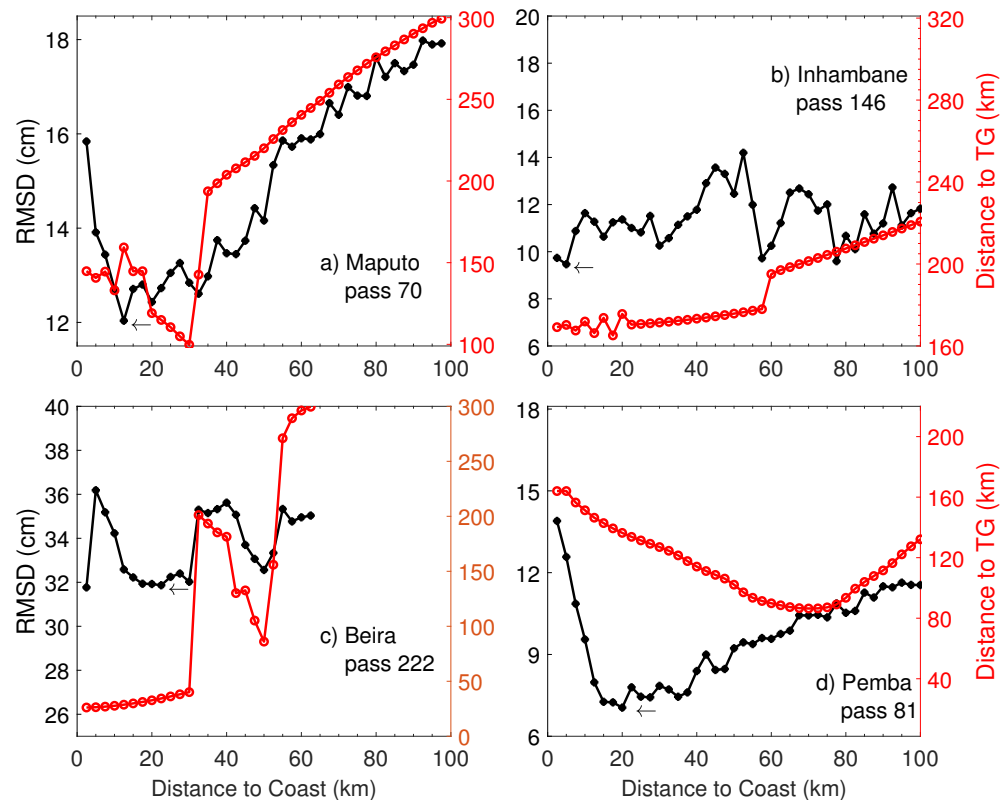
300 km from TG with a maximum temporal separation of 2 h were analyzed. The selection of satellite tracks with sea-level oscillations resembling those of the tide gauge was made through assessment of correlation coefficient and RMSD as a function of the distance from the coast.

Figure 2 presents the coefficient for the correlation between TG in the four sites and altimetric SSH, as a function of distance measured from the data point along the satellite track to the nearest point on the coast. The correlation coefficient in Beira was below 0.5 for all data points in all available tracks within the 300 km radius, and the TG data from the remaining three stations are well correlated with altimetry. As a first attempt, the altimetry data from pass number 70 were selected for further analysis at Maputo because they had the best correlation with TG data. For similar reasons, pass 222 was selected for Beira and pass 81 was selected for Pemba. In Inhambane, pass 5 gave the best correlation in spite of being located on land or exceedingly far away from the tide gauge. Alternatively, pass 196 was selected.



**Figure 2.** Correlation coefficient for Jason-series altimetry data computed for tracks located within 300 km from TG location in Maputo (a), Inhambane (b), Beira (c) and Pemba (d). Only the points located within 100 km from coast along satellite track are displayed.

Next, and for consistency, we inspected the RMSD, the position of the altimetry track in relation to the coastline and the distance from the altimetry data point to TG, ensuring that no selected track or data point along the track fell in a location that was by any means suspicious or had an unbearable error. The RMSD at the data points with the highest correlation was below 0.15 metres in all stations, as illustrated in Figure 3, with the exception of the Beira station, which displayed the largest root mean square difference of 0.32 metres. The satellite track 222 lies within 50 km from the TG station in Beira, and yet the datasets are poorly correlated, while in all other stations, the satellite tracks with the best correlation are located beyond a 100 km radius of the TG station.



**Figure 3.** Root mean square difference and distance to TG as functions of distance to coast for the selected satellite passes in Maputo (a), Inhambane (b), Beira (c) and Pemba (d). For reference, the position of data points giving the highest correlation is indicated by a left arrow. Notice the difference in limits of vertical axes in each panel.

Having selected the satellite tracks based on the correlation coefficient, we then moved to perform a closer investigation of the selected track, in search of a data point along the chosen track that would be better suited to perform further analysis. To that extent, the various altimetry data points at each TG station were distinguished by their correlation coefficient, and for each station, only the five data points with the highest correlation coefficient were assessed. The results are presented in Figure 4, where seven different metrics resulting from statistical analysis are shown, including measures of accuracy, precision and stability, the distance between TG and altimetric records and the number of matching pairs.

In Maputo (Figure 4a), the correlation coefficient varies between 0.59 and 0.62, and the closed contours are significantly different for each dataset. The greater temporal consistency indicated by smaller values of CV, the shorter distance to the tide gauge and the small root mean square difference justified the selection of data points located along track 146, for which the dataset gives the fifth highest correlation with TG data. The dataset with the maximum correlation belongs to track 70, and it is also associated with the largest error values for MAE and RMSD.

In Inhambane (Figure 4b), the correlation coefficient varies between 73.2% and 87.2% for the five datasets. The dataset showing the highest correlation is located along track 5 and was selected because it displays the largest temporal stability and smallest bias. However, it is the dataset located furthest apart from TG (i.e., 299.98 km) and with 13 MUs, it has the lowest number of matching pairs. The dataset located much closer to the TG for this station is roughly 170 km away along the pass 146, and it performs badly in all other metrics.

In Beira (Figure 4c), all altimetric datasets have a similar number of matching pairs, with those giving the top two correlation coefficients differing in temporal stability (i.e., CV) and performance. All five top correlations were found for track 222, yet none of the



data points have meaningful correlation ( $R > 0.50$ ), as their  $R$  values vary between 0.29 and 0.32. The dataset with the second highest correlation was selected because it shows better temporal stability, and numeric differences in other metrics are not so large. The selected point is located along pass 222 at 32.7 km from TG and has 38 matching pairs.

In Pemba (Figure 4d), the point along track 196 with the dataset with the second highest correlation was chosen mainly due to its shorter distance to TG, greater temporal stability and the largest number of matching pairs that allows the determination of robust statistics. Nonetheless, it should be noted that the selected dataset has a small bias and a small mean absolute error. The characteristics of all altimetry datasets selected for further analysis are summarized in Table 2.

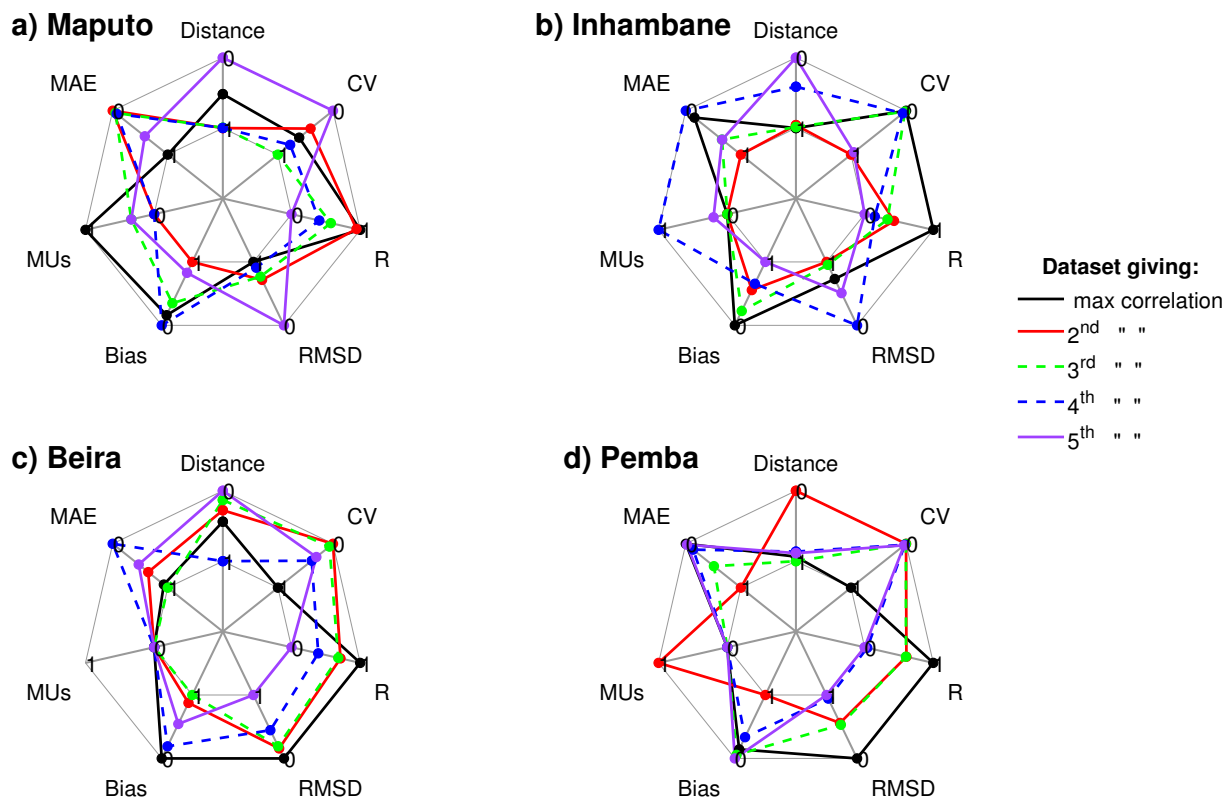


**Figure 4.** Comparison of seven metrics at the four TG stations, used to decide which altimetry dataset should be used in further analysis. Metrics are shown for Maputo (a), Inhambane (b), Beira (c), and Pemba (d), and they include distance to TG, coefficient of variance (CV), Pearson’s correlation coefficient (R), root mean square difference (RMSD), bias, number of match-ups (MUs) and mean absolute error (MAE). The center of each plot represents values that indicate a bad comparison for a particular altimetry dataset, while those farthest from the center represent the best agreement between altimetry and TG datasets. The data and limits of axes are normalized to the range of each metric.

**Table 2.** Parameters used to validate altimetry sea surface height.

	Maputo	Inhambane	Beira	Pemba
Altimetry pass	146	5	222	196
Number of Match-ups	63	13	38	110
Correlation coefficient	0.59	0.87	0.31	0.75
RMSD, cm	11.36	10.53	31.92	7.27
MAE, cm	9.57	8.04	23.93	10.49
Bias, cm	−1.95	1.33	−4.66	7.02
Coefficient of variance	−1.26	−2.45	−2.34	1.12
Distance to coast, km	18.79	10.09	18.70	15.40
Distance to TG, km	83.75	299.98	32.70	42.45

### 3.2. Time Series Analysis

Figure 5 shows the time-series sea surface height anomaly (SSHA) for selected altimetry points and passes, along with TG observations. There are huge gaps clearly visible in the four datasets, and particularly for Inhambane, the data cover only 300 days of the year 2011. Given the 9.9156-day repeat period of the Jason satellites, the 300 days result in only 30 valid points for TG/Altimetry inter-comparison, and this reduces even further to 13 matching units after the removal of outliers and those data with temporal separation surpassing 2 h. Even in locations with a large number of matching points, data gaps covering long periods are found, posing a problem for the determination of robust statistics. A visual inspection of the graphs indicates that altimetry data seem to agree more with TG data in Pemba, followed by the Inhambane station. TG data in these two stations are processed and archived at UHSLC, whilst the other two stations with smaller correlation coefficients and poorer visible agreement are distributed by IOC-SLMF. While Pemba and Maputo stations have the longest timeseries and more matching pairs, Inhambane has the best correlation despite its shorter timeseries and fewer matching pairs.

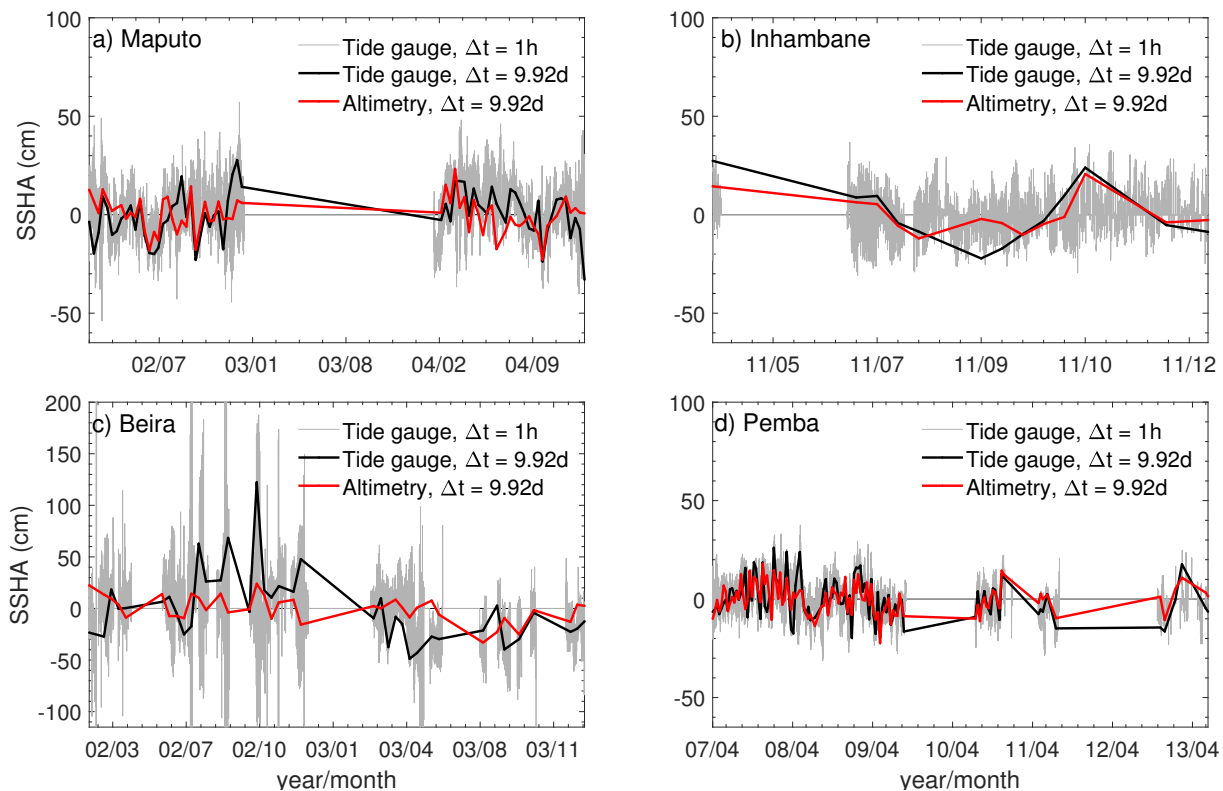


**Figure 5.** Time series of de-tided sea level from altimetry observations (red) for the satellite passes depicted in Table 2 and tide gauge (black) at the four locations. The sampling interval for the observations is nearly 10 days. The time series of sea-surface height anomalies from tide gauge at the original sampling interval of 1 h (gray) is also shown for reference.

Table 3 presents the amplitude and phase of the annual and semi-annual cycles of sea level estimated from collocated satellite altimetry and tide gauge datasets. Maximum and minimum values from the de-seasoned and de-trended time series (i.e., the term  $\epsilon_t$  in Equation (3)) over the entire period covered by either the tide gauge or the altimetry data are also shown as a measure of the variability. When comparing the annual amplitude in the two datasets, one finds that the TG to altimetry difference is roughly  $-2.1$ ,  $+40$ ,  $+19$  and  $+0.2$  cm for Maputo, Inhambane, Beira and Pemba stations. In the same order of stations, the difference in the annual phase lag is  $+114$ ,  $+5$ ,  $+265$  and  $+10$  days. These differences are an indication that the annual cycle from altimetry is, in general, smaller and ahead of TG by a few days in Inhambane and Pemba, and by many months in the remaining two

stations. Likewise, for the semi-annual cycles, the differences are +2, +25, +2 and +2 cm in amplitude, and +77, +3, −76, −40 days in phase. Again, the amplitude of the semi-annual cycle from altimetry is smaller than TG in all stations, and while this cycle lags behind TG in Maputo and Inhambane, it is ahead of TG in Beira and Pemba. It should be noted that both the annual and semi-annual cycles are far more comparable in Pemba, where the amplitude in particular has the same order of magnitude, and the Maputo station comes in second.

**Table 3.** Amplitude and phase of the annual and semi-annual sea-level cycles, as estimated from satellite altimetry and tide gauge at the four locations. Errors denote one standard error derived using Bayesian regression with auto-correlated errors. There is not enough data points (i.e., matching pairs) to compute robust statistics for Inhambane.

	Maputo		Inhambane	
	Altimetry	Tide Gauge	Altimetry	Tide Gauge
Annual amplitude, cm	6.8 ± 1.5	4.7 ± 2.6	90.1 ± 54.1	132.6 ± 65.9
Annual phase, days	41.5 ± 11.9	155.9 ± 111.2	153.7 ± 66.4	158.1 ± 39.9
Semi-annual amplit., cm	2.3 ± 1.1	4.6 ± 2.5	33.0 ± 16.2	58.1 ± 17.5
Semi-annual phase, days	55.7 ± 26.8	133.2 ± 42.0	125.8 ± 21.8	128.8 ± 10.5
Max anomaly, cm	11.1	28.4	12.2	18.9
Min anomaly, cm	−12.8	−32.5	−16.0	−27.1
	Beira		Pemba	
	Altimetry	Tide Gauge	Altimetry	Tide Gauge
Annual amplitude, cm	5.7 ± 3.0	24.8 ± 6.4	4.7 ± 1.0	4.5 ± 1.3
Annual phase, cm	36.4 ± 59.3	301.5 ± 21.3	5.7 ± 13.3	14.6 ± 20
Semi-annual amplit., cm	4.5 ± 2.5	6.5 ± 5.3	1.3 ± 0.7	3.2 ± 1.2
Semi-annual phase, days	134.6 ± 41.2	54.8 ± 46.8	100.7 ± 44.6	61.1 ± 15.8
Max anomaly, cm	21.1	90.8	11.2	27.3
Min anomaly, cm	−25.4	−48.8	−12.2	−24.6

In all four stations, the maximum and minimum anomalies are considerably larger in magnitude for TG observations compared to satellite altimetry, with the Beira station having the largest differences. This suggests that part of altimetry results in a de-seasoned and de-trended time-series is consistently reduced in magnitude.

#### 4. Discussion

In this study, along-track satellite altimetry data from the Jason series of satellites reprocessed with the ALES re-tracker were compared against tide gauge data. The in situ data measurements are part of the national sea-level monitoring program of Mozambique in the western Indian Ocean, which comprises thirteen TG stations, including five operational stations that are spread over the country’s 2700 km-long coastline. The monitoring of sea level is performed erratically in all stations due to lack of equipment, difficulty acquiring replacement parts, lack of qualified maintenance personnel, lack of funds to maintain tide gauges and difficulty accessing remote tide gauges due to insurgency [14]. The need to comprehend the extent to which sea-level rise impacts physical structures, as well as living and non-living resources throughout the coast, is well recognized in the Mozambique Marine Spatial Plan [38]. The country’s capacity to adequately use satellite products and mainstream their outputs into risk management policies, including those associated with extreme events and sea-level change, is somewhat deficient. Not to mention the lack of altimetry algorithms known to perform well in coastal waters combined with the existing set of inconsistent TG observations, which makes it difficult—if not impossible—to monitor long-term trends in sea level along the coasts of Mozambique. Some of these tools are mandatory when climate-change-associated future changes are to be predicted and management measures for coastal risks are to be devised. With that in mind, we set out to validate the ALES re-tracked altimetric measurements against TG data obtained from four ground stations.

Outputs of the ALES re-tracker have been previously validated in other parts of the world [7,13,34], where the algorithm showed constant and good agreement with in situ

data (correlation coefficient,  $R > 80\%$ ), compared with other available algorithms designed for the open ocean. These authors indicated that the correlation for ALES output in coastal regions is consistently above 60% when the Jason-1 and Jason-2 data are used in particular.

In the results presented here, the correlation coefficient varied to some degree across the four TG stations. While in Maputo, Inhambane and Pemba, the R-values were positive throughout the 100 km from the coast, with strong correlations ( $R > 0.50$ ) at some points, Beira showed R-values with positive and negative signs, and correlation was weak for all satellite passes considered. There is a clear tendency for R-values to increase exponentially from the coastline to an offshore distance of about 20 km, from which it decreases linearly with distance. This pattern is much more pronounced for passes in Maputo and Pemba, where the distance to the coast increases almost linearly seawards. An enhanced altimetry performance in the 5–20 km coastal ocean fringe had been previously reported in [39,40], and these authors also suggested that altimetry performance is somehow related to the flight direction during land–ocean transition of the satellite track, the orientation of the coastline with respect to the track, and the coastal topography near the altimetry footprint. Moreover, the use of altimetry data in coastal ocean application relies on our ability to remove or mitigate unwanted effects caused by the atmosphere, ocean, land and the instrument, including their algorithms for retrieving meaningful information. ALES was presented as a means to overcome difficulties that include “jumps” in the retrieved parameters resulting from the different coastal conditions, numerical convergence in parameter estimation, the switch between different re-trackers (i.e., for open ocean and coast) and a few others [10]. However, some issues are still not resolved in this algorithm, such as the transition from land to ocean; therefore, it seems reasonable to assume that some of the variance observed in this study is due to the mere application of ALES in this particular coastal region and the choice of corrections in the C-RISe dataset that includes the “global” FES2014 Ocean Tide model.

For the satellite tracks containing data with the highest correlation coefficient, the data points with the lowest RMSD are located within 25 km from the coast, close enough to the coast yet not the closest, and quite often they are far from the TG stations. This pattern is consistent with the findings in [7] and [32], and it suggests that the weak correlation in Beira could be associated with factors other than the position of the satellite track and its points, nor with the capabilities of the ALES re-tracker. These local factors could include inconsistencies in the TG time-series, exposure of TG to unresolved wave action constrained by local bathymetry [39], background noise such as mesoscale ocean variability [41] and the occurrence of storm surges. The central coast of Mozambique (i.e., in the vicinity of Beira station) is where most of the tropical storms and cyclones make landfall, and the most severe of those systems have a larger contribution of the atmospheric sea-level pressure surpassing the contribution of the tide-surge nonlinear interactions [42].

A variety of performance metrics can be found in the literature, metrics that are commonly used for validation of earth observation data or other inter-comparison of datasets. A succinct review is presented in [37], who also pointed that the choice of metrics used in the validation process depends on the intended application of the products [36], as well as the data availability [43]. With that in mind, and considering our immediate goal of characterizing the sea-level anomalies at the four coastal locations for which in situ data was made available, despite its irregular sampling and short timespan, five other metrics were analyzed. The number of matching pairs, which gives a coarse estimate of collocation uncertainty, was used to determine whether or not the dataset could be used to calculate robust regressions.

Earlier attempts to validate altimetry data indicated that the performance of altimetry reduced significantly very close to the coast [8], since tide gauge readings there used to compare with altimetry are dominated by coastal processes that are rarely captured by satellites, unless they are taken a few kilometres from the tide gauge. The altimetry data used here (Table 2) are located within 20 km from the coast, yet very far from the TG station, still indicating a great performance of the ALES re-tracker. This also points to

room for improvement in either the re-tracker algorithm or the procedures employed in the validation, with the spatio-temporal collocation being one of the major shortcomings. In our approach, the data were kept on their original grid and time, and then the closest matches were selected, whilst a few other methods are proposed in the literature, mainly for satellite imagery, that involve statistically assessing the data representativeness [44], bringing both datasets onto the same grid and temporal scale by various means [37], and performing indirect validation by adding a few more data points for the match-up, thereby undertaking triple or multi-collocation [45,46]. However, regardless of the collocation method employed, a residual uncertainty will always be present, and its evaluation was the premise for development of the triple collocation methods.

The subjective analysis of additional metrics presented in Figure 4 indicated primarily that a single criteria cannot be applied for multiple sites. Instead, each site needs a separate evaluation that includes both a quantitative and qualitative appraisal of the metrics. It has been suggested that when selecting performance metrics the user considerations should include the impact of: (i) outliers; (ii) the full range of the data versus a specific and narrow data range; (iii) the temporal and/or spatial stability of an algorithm; (iv) the spatial coverage provided by an algorithm; (v) allowable uncertainties; and (vi) allowable biases [47]. In the present analysis, we elicited strong agreement between satellite and in situ data (e.g., positive  $R > 0.50$  or the highest available), a good temporal consistency of time-series (e.g., CV as close to zero as possible), and a small bias yet without a threshold as those defined the satellite dataset better compared to the TG, and used those to compute statistics for the observed sea level. Following [37], the chosen metrics are sensitive to either two forms of random measurement uncertainty, random representativeness difference and systematic representativeness differences, which indicates that inaccuracies resulting from the application of these metrics are similar for the remaining metrics, and most importantly, they are inherent to the sampling techniques applied both in altimetry and in situ gauge. In particular, the in situ gauge data are subjected to a long list of sources of error, and not all of them can be corrected during a quality control process.

The amplitudes and phases of the annual and semi-annual cycles varied considerably in each of the four locations, both in altimetry and TG datasets. This geographical non-uniformity is not uncommon, as [12] found similar pattern in a number of stations in the United Kingdom. In general, the amplitude of the annual cycle is one to three times larger than that of the semi-annual cycle, and the agreement between altimetry and TG is good, with both datasets having the same order of magnitude. Inhambane and Beira stations constitute an exception, most likely due to inconsistencies in the TG records. The anomalies in the altimetry dataset presented here vary from just a few to almost 30 centimetres in all four stations, in agreement with [7], though it must be noted that the Beira station is located in a macro-tidal environment with large deviations from the mean anomaly presented in Figure 5. With the 10-day resampling period imposed on the TG data, most of these large anomalies are dampened to a maximum of  $\sim 90$  cm, resulting in the largest values of RMSD and MAE. This makes it impossible to validate the altimetry data at this station. On the other hand, this study concluded that the altimetry data from the Jason series of satellites reprocessed with the ALES re-tracker offers a cost-effective way of taking sea-level measurements in Maputo, Inhambane and Pemba, albeit with the reservation that the collocation technique needs to be improved and in situ observations need to be more consistent in order to acquire the level of agreement reported for other locations.

A good understanding of all coastal hazards related to sea level requires long-term, high-quality observations, which according to [48] can only be assured through dedicated funding and skilled local operators. We have demonstrated here that satellite altimetry for Maputo, Inhambane and Pemba provides valid data that can be used to improve the regional information on coastal risk factors, therefore supporting the development of improved plans to protect coastal communities, ecosystems and economic activity. These coastal cities are exposed to storm surges associated with tropical cyclones, which often leads to enhanced coastal erosion, overtopping and flooding [38]. The frequency, magni-



tude and impacts of the processes with potential to a coastal hazard vary largely in time and space, mirroring the diverse geomorphological constraints as well as oceanographic forcing constraints.

## 5. Conclusions

In this study, altimetry data reprocessed with the ALES coastal re-tracker were compared with the tide observations, in order to check the suitability of the data for the assessment of coastal risks in Mozambique. The study provides validation for the long-term, consistent, free-of-charge altimetry data, and expands the geographical area of applicability of the ALES processor.

Sea surface height anomaly shows a correlation coefficient of 0.59, 0.87 and 0.75 for the agreement between in situ TG observations and altimetric data points located within 10–20 km from the coast in Maputo, Inhambane, and Pemba, respectively. In addition, in Maputo and Pemba, the amplitude of annual and semi-annual cycles of the de-tided and de-trended sea level has the same order of magnitude in both altimetry and TG data, with the annual cycle being twice as large as the semi-annual. No general agreement was found for the phase difference across stations.

The study also concluded that a much more consistent time-series from Beira TG (e.g., continuous if possible and spanning a longer period) is needed in order to appropriately validate the satellite altimetry data, and make it possible to combine altimetry and tide gauge data to enhance knowledge of coastal sea level and how it is changing, so that lives, infrastructure and livelihoods can be protected.

**Author Contributions:** Conceptualization, F.P.J.N., P.D.C. and A.H.; methodology, A.H., C.M.; software, F.C.; validation, Z.D.H.V., F.P.J.N., C.M. and A.H.; formal analysis, Z.D.H.V.; investigation, F.P.J.N.; resources, P.D.C.; writing—original draft preparation, F.P.J.N.; writing—review and editing, P.D.C.; visualization, F.P.J.N.; supervision, F.P.J.N.; project administration, P.D.C.; funding acquisition, P.D.C. All authors have read and agreed to the published version of the manuscript.

**Funding:** This study is part of the Coastal Risk Information Service (C-RISe) project that was funded by the UK Space Agency (UKSA) under the International Partnership Programme.

**Institutional Review Board Statement:** Not applicable.

**Informed Consent Statement:** Not applicable.

**Acknowledgments:** We acknowledge the SatOc and ESCMC-UEM staff for their administrative support, and NOC staff for their technical support.

**Conflicts of Interest:** The authors declare no conflicts of interest. The funders had no role in the design of the study; in the collection, analyses, or interpretation of data; in the writing of the manuscript, or in the decision to publish the results.

## References

1. Gornitz, V. Global coastal hazards from future sea level rise. *Palaeogeogr. Palaeoclimatol. Palaeoecol.* **1991**, *89*, 379–398. [[CrossRef](#)]
2. Hauer, M.E.; Evans, J.M.; Mishra, D.R. Millions projected to be at risk from sea-level rise in the continental United States. *Nat. Clim. Change* **2016**, *6*, 691–695. [[CrossRef](#)]
3. Cazenave, A.; Dominh, K.; Ponchaut, F.; Soudarin, L.; Cretaux, J.F.; Le Provost, C. Sea level changes from Topex-Poseidon altimetry and tide gauges, and vertical crustal motions from DORIS. *Geophys. Res. Lett.* **1999**, *26*, 2077–2080. [[CrossRef](#)]
4. Cazenave, A.; Cabanes, C.; Dominh, K.; Gennero, M.C.; Le Provost, C. Present-day sea level change: Observations and causes. *Space Sci. Rev.* **2003**, *108*, 131–144. [[CrossRef](#)]
5. Melet, A.; Teatini, P.; Le Cozannet, G.; Jamet, C.; Conversi, A.; Benveniste, J.; Almar, R. Earth observations for monitoring marine coastal hazards and their drivers. *Surv. Geophys.* **2020**, *41*, 1489–1534. [[CrossRef](#)]
6. Cipollini, P.; Benveniste, J.; Birol, F.; Fernandes, M.J.; Obligis, E.; Passaro, M.; Strub, P.T.; Valladeau, G.; Vignudelli, S.; Wilkin J. Satellite Altimetry in Coastal Regions. In *Satellite Altimetry Over Oceans and Land Surfaces*; Stammer, D., Cazenave, A., Eds.; CRC Press: Boca Raton, FL, USA, 2017; pp. 343–380.
7. Passaro, M.; Cipollini, P.; Vignudelli, S.; Quartly, G.D.; Snaith, H.M. ALES: A multi-mission adaptive subwaveform retracker for coastal and open ocean altimetry. *Remote Sens. Environ.* **2014**, *145*, 173–189. [[CrossRef](#)]

8. Benveniste, J.; Cazenave, A.; Vignudelli, S.; Fenoglio-Marc, L.; Shah, R.; Almar, R.; Andersen, O.; Birol, F.; Bonnefond, P.; Bouffard, J.; et al. Requirements for a coastal hazards observing system. *Front. Mar. Sci.* **2019**, *6*, 348. [[CrossRef](#)]
9. Nehama, F.P.J.; Matavel, A.J.; Hogueane, A.M.; Menomussanga, M.; Hogueane, C.A.M.; Zacarias, O.; Lemos, M.A. Building community resilience and strengthening local capacities for disaster risk reduction and climate change adaptation in Zongoene (Xai-Xai District), Gaza Province. In *Climate Change and Health*; Filho, W.L., Azeiteiro, U.M., Alves F., Eds.; Springer: Cham, Switzerland, 2015; pp. 369–385.
10. Mavume, A.F.; Rydberg, L.; Rouault, M.; Lutjeharms, J.R. Climatology and landfall of tropical cyclones in the south-west Indian Ocean. *West. Indian Ocean J. Mar. Sci.* **2009**, *8*, 15–36. [[CrossRef](#)]
11. C-RiSe. Importance of Coastal Sea Level Monitoring for Mozambique. Summary for Policy Makers. Technical Report 2021. Available online: <https://www.c-rise.info> (accessed on 15 April 2019).
12. Cipollini, P.; Calafat, F.M.; Jevrejeva, S.; Melet, A.; Prandi, P. Monitoring Sea Level in the Coastal Zone with Satellite Altimetry and Tide Gauges. *Surv. Geophys.* **2017**, *38*, 33–57. [[CrossRef](#)]
13. Gómez-Enri, J.; Vignudelli, S.; Quartly, G.D.; Gommenginger, C.P.; Cipollini, P.; Challenor, P.G.; Benveniste, J. Modeling Envisat RA-2 waveforms in the coastal zone: Case study of calm water contamination. *IEEE Geosci. Remote Sens. Lett.* **2010**, *7*, 474–478. [[CrossRef](#)]
14. Wang, X.; Ichikawa, K. Coastal waveform retracking for Jason-2 altimeter data based on along-track Echograms around the Tsushima Islands in Japan. *Remote Sens.* **2017**, *9*, 762. [[CrossRef](#)]
15. Kolstad, E.W. Prediction and precursors of Idai and 38 other tropical cyclones and storms in the Mozambique Channel. *Q. J. R. Meteorol. Soc.* **2021**, *147*, 45–57. [[CrossRef](#)]
16. Atkinson, G.D.; Holliday, C.R. *Tropical Cyclone Minimum Sea Level Pressure-Maximum Sustained Wind Relationship for Western North Pacific*; Technical Report; US Fleet Weather Central Guam: San Francisco, CA, USA, 1975.
17. Pugh, D.T. *Tides, Surges and Mean Sea Level*; John Wiley and Sons Inc.: New York, NY, USA, 1987.
18. Chevane, C.M.; Penven, P.; Nehama, F.P.J.; Reason, C.J.C. Modelling the tides and their impacts on the vertical stratification over the Sofala Bank, Mozambique. *Afr. J. Mar. Sci.* **2016**, *38*, 465–479. [[CrossRef](#)]
19. Malauene, B.S.; Shillington, F.A.; Roberts, M.J.; Moloney, C.L. Cool, elevated chlorophyll-a waters off northern Mozambique. *Deep Sea Res. Part II Top. Stud. Oceanogr.* **2014**, *100*, 68–78. [[CrossRef](#)]
20. Vinayachandran, P.N.M.; Masumoto, Y.; Roberts, M.J.; Huggett, J.A.; Halo, I.; Chatterjee, A.; Amol, P.; Gupta, G.; Singh, A.; Mukherjee, A.; et al. Reviews and syntheses: Physical and biogeochemical processes associated with upwelling in the Indian Ocean. *Biogeosciences* **2021**, *18*, 5967–6029. [[CrossRef](#)]
21. Cossa, O.; Pous, S.; Penven, P.; Capet, X.; Reason, C.J.C. Modelling cyclonic eddies in the Delagoa Bight region. *Cont. Shelf Res.* **2016**, *119*, 14–29. [[CrossRef](#)]
22. da Silva, J.C.B.; New, A.L.; Magalhaes, J.M. Internal solitary waves in the Mozambique Channel: Observations and interpretation. *J. Geophys. Res.* **2009**, *14*, C05001. [[CrossRef](#)]
23. Sigaúque, P.J.; Schettini, C.A.F.; Valentim, S.S.; Siegle, E. The role of tides, river discharge and wind on the residual circulation of Maputo Bay. *Reg. Stud. Mar. Sci.* **2021**, *41*, 101604. [[CrossRef](#)]
24. Canhanga, S.; Dias, J.M. Tidal characteristics of Maputo bay, Mozambique. *J. Mar. Syst.* **2005**, *58*, 83–97. [[CrossRef](#)]
25. Lencart e Silva, J.D.; Simpson, J.H.; Hogueane, A.M.; Harcourt-Baldwin, J.-L. Buoyancy-stirring interactions in a subtropical embayment: A synthesis of measurements and model simulations in Maputo Bay, Mozambique. *Afr. J. Mar. Sci.* **2010**, *32*, 95–107. [[CrossRef](#)]
26. Solana, G.; Grifoll, M.; Espino, M. Hydrographic variability and estuarine classification of Inhambane Bay (Mozambique). *J. Coast. Res.* **2020**, *95*, 649–653. [[CrossRef](#)]
27. Nzualo, T.N.M. Estudo hidrodinâmico e Ambiental do Estuário da Beira-Moçambique. Master's Thesis, Universidade Federal do Rio de Janeiro, Rio de Janeiro, Brazil, 2010.
28. Sete, C. Tides Structures and Mixing Along the Mozambique Coast. Master's Thesis, University of Bergen, Bergen, Norway, 2010.
29. Andersen, O.B.; Stenseng, L.; Piccioni, G.; Knudsen, P. The DTU15 MSS (Mean Sea Surface) and DTU15LAT (Lowest Astronomical Tide) reference surface. In Proceedings of the ESA Living Planet Symposium 2016, Prague, Czech Republic, 9–13 May 2016.
30. Flanders Marine Institute (VLIZ). Intergovernmental Oceanographic Commission (IOC) (2021): Sea Level Station Monitoring Facility. Available online: <http://www.ioc-sealevelmonitoring.org> (accessed on 22 May 2021).
31. Passaro, M.; Rose, S.K.; Andersen, O.B.; Boergens, E.; Calafat, F.M.; Dettmering, D.; Benveniste, J. ALES+: Adapting a homogenous ocean retracker for satellite altimetry to sea ice leads, coastal and inland waters. *Remote Sens. Environ.* **2018**, *211*, 456–471. [[CrossRef](#)]
32. Vu, P.L.; Frappart, F.; Darrozes, J.; Marieu, V.; Blarel, F.; Ramillien G.; Bonnefond, P.; Birol, F. Multi-Satellite Altimeter Validation along the French Atlantic Coast in the Southern Bay of Biscay from ERS-2 to SARAL. *Remote Sens.* **2018**, *10*, 93. [[CrossRef](#)]
33. Taqi, A.M.; Al-Subhi, A.M.; Alsaafani, M.A.; Abdulla, C.P. Improving Sea Level Anomaly Precision from Satellite Altimetry Using Parameter Correction in the Red Sea. *Remote Sens.* **2020**, *12*, 764. [[CrossRef](#)]
34. Xu, X.-Y.; Birol, F.; Cazenave, A. Evaluation of Coastal Sea Level Offshore Hong Kong from Jason-2 Altimetry. *Remote Sens.* **2018**, *10*, 282. [[CrossRef](#)]
35. Carrere, L.; Faugère, Y.; Ablain, M. Major improvement of altimetry sea level estimations using pressure-derived corrections based on ERA-Interim atmospheric reanalysis. *Ocean Sci* **2016**, *12*, 825–842. [[CrossRef](#)]

36. Seegers, B.N.; Stumpf, R.P.; Schaeffer, B.A.; Loftin, K.A.; Werdell, P.J. Performance metrics for the assessment of satellite data products: An ocean color case study. *Opt. Express* **2018**, *26*, 7404–7422. [[CrossRef](#)]
37. Loew, A.; Bell, W.; Brocca, L.; Bulgin, C.E.; Burdanowitz, J.; Calbet, X.; Reik, V.; Donner, R.V.; Ghent, D.; Gruber, A.; et al. Validation practices for satellite-based Earth observation data across communities. *Rev. Geophys.* **2017**, *55*, 779–817. [[CrossRef](#)]
38. MIMAIP. Elaboração do Plano de Ordenamento do Espaço Marítimo (POEM)—Fase 2—Inventário e Caracterização. Caracterização Geral. Technical Report. 2020; Ministério do Mar, Águas Interiores e Pescas. Available online: <https://poem.gov.mz> (accessed on 15 July 2022).
39. Aldarias, A.; Gómez-Enri, J.; Laiz, I.; Tejedor, B.; Vignudelli, S.; Cipollini, P. Validation of Sentinel-3A SRAL Coastal Sea Level Data at High Posting Rate: 80 Hz *IEEE Trans. Geosci. Remote Sens.* **2020**, *58*, 3809–3821. [[CrossRef](#)]
40. Piccioni, G.; Dettmering, D.; Passaro, M.; Schwatke, C. Coastal Improvements for Tide Models: The Impact of ALES Retracker. *Remote Sens.* **2018**, *10*, 2072–4292. [[CrossRef](#)]
41. Pan, H.; Devlin, A.T.; Xu, T.; Lv, X.; Wei, Z. Anomalous 18.61-Year Nodal Cycles in the Gulf of Tonkin Revealed by Tide Gauges and Satellite Altimeter Records. *Remote Sens.* **2022**, *14*, 3672. [[CrossRef](#)]
42. Bié, A.J.; Camargo, R.; Mavume, A.F.; Harari, J. Numerical modeling of storm surges in the coast of Mozambique: The cases of tropical cyclones Bonita (1996) and Lisette (1997). *Ocean Dyn.* **2017**, *67*, 1443–1459. [[CrossRef](#)]
43. Muraleedharan, P.M.; Pankajakshan, T. An interactive software package for validating satellite data. *Gayana (Concepción)* **2004**, *68*, 411–419. [[CrossRef](#)]
44. Román, M.O.; Schaaf, C.B.; Woodcock, C.E.; Strahler, A.H.; Yang, X.; Braswell, R.H.; Curtis, P.S.; Davis, K.J.; Dragoni, D.; Goulden, M.L. The MODIS (Collection V005) BRDF/albedo product: Assessment of spatial representativeness over forested landscapes *J. Remote Sens. Environ.* **2009**, *113*, 2476–2498. [[CrossRef](#)]
45. Jiang, H. Indirect validation of ocean remote sensing data via numerical model: An example of wave heights from altimeter. *Remote Sens.* **2020**, *12*, 2627. [[CrossRef](#)]
46. Schulz-Stellenfleth, J.; Staneva, J. A multi-collocation method for coastal zone observations with applications to Sentinel-3A altimeter wave height data. *Ocean Sci.* **2019**, *15*, 249–268. [[CrossRef](#)]
47. Armstrong, J.S. Evaluating Forecasting Methods. In *Principles of Forecasting*; Armstrong, J.S., Ed.; International Series in Operations Research and Management Science; Springer: Boston, MA, USA, 1987; Volume 30.
48. Hibbert, A. Building resilience to coastal hazards using tide gauges. *Environ. Sci.* **2021**, 58–65.